

in Refs. 5 and 6 have similar structure at low excitation energies: They are all characterized by well-developed rotational bands with backbending in the even systems and with strongly populated partly decoupled positive-parity bands in the odd ones. Also the input angular momenta in all these works are similar. As far as the deformed rare-earth nuclides are concerned, the present result implies that there is no solid experimental evidence for "the existence of a small-deformation oblate region" at high spin values, as inferred from intense low-energy  $M1$  transitions in a semiphenomenological theoretical approach.<sup>8</sup> No such statement can be made about the results of Ref. 2, which concerned lighter nuclei near closed shells studied at significantly higher angular-momentum input than in this work. Such nuclei are expected to acquire oblate deformed shapes at high spins and therefore to exhibit quite a different pattern of electromagnetic radiation than that characteristic for the prolate deformed nuclei.

This work was performed as part of the research program of the Stichting voor Fundamenteel Onderzoek der Materie (FOM) with financial support from the Nederlandse Organisatie voor Zuiver Wetenschappelijk Onderzoek (ZWO).

<sup>(a)</sup>On leave from the Institut de Physique Corpusculaire, Louvain-la-Neuve, Belgium.

<sup>1</sup>M. V. Banaschik, R. S. Simon, P. Colombani, D. P. Soroka, F. S. Stephens, and R. M. Diamond, *Phys. Rev. Lett.* **34**, 892 (1975).

<sup>2</sup>M. A. Deleplanque, T. Byrski, R. M. Diamond, H. Hübel, F. S. Stephens, B. Herskind, and R. Bauer, *Phys. Rev. Lett.* **41**, 1105 (1978).

<sup>3</sup>S. J. Feenstra, W. J. Ockels, J. van Klinken, M. J. A. de Voigt, and Z. Sujkowski, *Phys. Lett.* **69B**, 403 (1977).

<sup>4</sup>S. J. Feenstra, J. van Klinken, J. P. Pijn, R. Janssens, C. Michel, J. Steyaert, J. Vervier, K. Cornelis, M. Huyse, and G. Lhersonneau, *Phys. Lett.* **80B**, 183 (1979).

<sup>5</sup>L. Westerberg, D. G. Sarantites, K. Geoffroy, R. A. Dayras, J. R. Beene, M. L. Halbert, D. C. Hensley, and J. H. Barker, *Phys. Rev. Lett.* **41**, 96 (1978).

<sup>6</sup>J. O. Newton, S. H. Sie, and G. D. Dracoulis, *Phys. Rev. Lett.* **40**, 625 (1978).

<sup>7</sup>S. M. Ferguson, H. Ejiri, and I. Halpern, *Nucl. Phys.* **188**, 1 (1972).

<sup>8</sup>L. K. Peker, J. H. Hamilton, and J. O. Rasmussen, *Phys. Rev. Lett.* **41**, 457 (1978).

<sup>9</sup>D. Chmielewska, Z. Sujkowski, J. F. W. Jansen, W. J. Ockels, and M. J. A. de Voigt, *Nukleonika* **23**, 233 (1978), and **24**, 395 (1979).

<sup>10</sup>W. J. Ockels, M. J. A. de Voigt, and Z. Sujkowski, *Phys. Lett.* **78B**, 401 (1978), and to be published.

## Evidence for Rotational Structure at High Spins in <sup>154,155</sup>Er

M. A. Deleplanque, J. P. Husson, N. Perrin, and F. S. Stephens  
*Institut de Physique Nucléaire, F-91406 Orsay, France*

and

G. Bastin, C. Schüeck, and J. P. Thibaud  
*Centre de Spectrométrie Nucléaire et de Spectrométrie de Masse, F-91406 Orsay, France*

and

L. Hildingsson, S. Hjorth, A. Johnson, and Th. Lindblad  
*Research Institute of Physics, S-10405 Stockholm, Sweden*

(Received 22 May 1979)

Erbium nuclei around  $N=86$ , which are weakly collective at spins below about  $40\hbar$ , have been studied at higher spin using techniques recently developed for studying continuum  $\gamma$  rays. A strong collective structure appears to develop above spins around  $40\hbar$ , which can explain why no discrete lines have been observed beyond  $36\hbar$ . The similarity of the spectra for heavier and lighter erbium nuclei at spins  $(40-60)\hbar$  suggests the same shape (prolate) for both.

Recently, the level schemes of several nuclei<sup>1</sup> just above the  $N=82$  shell have been determined up to very high spins (about  $40\hbar$ ). All these nuclei are characterized by an irregular weakly

collective yrast band which is heavily populated. No discrete lines due to transitions above spin  $36\hbar$  are seen, probably because many parallel cascades are here involved in the  $\gamma$ -ray deexcita-

tion of the nucleus. These  $\gamma$  rays then form an unresolved "continuum" which can be studied by methods which have been recently developed. The multiplicity spectra<sup>2</sup> (number of coincident  $\gamma$  rays as a function of  $\gamma$ -ray energy) can indicate if there is a correlation between the  $\gamma$ -ray transition energy and spin and also can locate those  $\gamma$ -ray transitions coming from the highest spins populated. The multipole spectra<sup>3</sup> (a separate spectrum for each transition multipole type) can be constructed from the angular distribution of the continuum  $\gamma$  rays. The purpose of the present work is to learn about higher spins in the nuclei around  $N=86$  by applying these methods.

Previously, these continuum studies have been made following compound-nucleus reactions, but without selection of the final product nucleus. In the present experiment, such a selection is made possible by the inclusion of a Ge(Li) detector in the experimental setup. The complete detector arrangement is shown in Fig. 1. We placed two 7.5-cm  $\times$  7.5-cm NaI detectors 60 cm from the target, at angles of  $0^\circ$  and  $90^\circ$  with respect to the beam direction, and in addition there was a Ge(Li) detector located above the target, 12.5 cm away. Both singles [without Ge(Li)] events and Ge(Li) coincident events have been recorded, in coincidence with a multiplicity filter. This filter consisted of six 7.5-cm  $\times$  7.5-cm NaI counters located in a circle in the horizontal plane, 14 cm from the target. All the NaI spectra have been unfolded, using methods previously described.<sup>4</sup> The system  $^{124}\text{Sn} + ^{40}\text{Ar}$  leading to residual nuclei well known to be rotational up to the highest spins observed (around  $60\hbar$ ) has been compared to the system  $^{119}\text{Sn} + ^{40}\text{Ar}$  leading to the nuclei around  $N=86$  which are weakly collective at low spins.

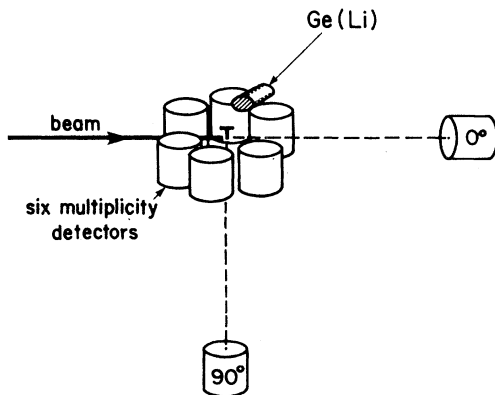


FIG. 1. Experimental setup.

The Ar beam has been produced at the ALICE facility in Orsay, at 170 and 183 MeV for the  $^{124}\text{Sn}$  and the  $^{119}\text{Sn}$  systems, respectively, in order to give approximately equal  $4n$  and  $5n$  cross sections in each case.

Figure 2(a) compares the fourfold singles spectra [i.e., in coincidence with any four of the multiplicity detectors, but not with the Ge(Li) detector] for the  $0^\circ$  detector from the  $^{124}\text{Sn}$  and  $^{119}\text{Sn}$  targets, normalized to the same exponential tail. The  $^{164}\text{Er}$  compound nucleus (mainly  $^{160}\text{Er}$  and

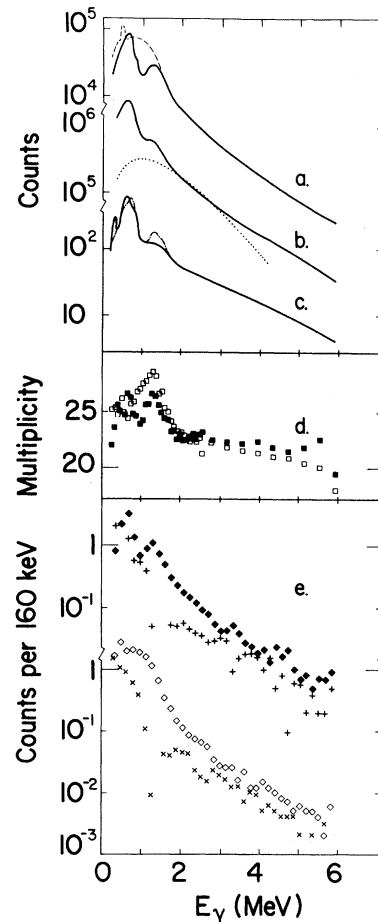


FIG. 2. (a) Fourfold  $0^\circ$  singles spectra for  $^{124}\text{Sn} + ^{40}\text{Ar}$  system (dashed line) and  $^{119}\text{Sn} + ^{40}\text{Ar}$  system (solid line). (b) Experimental spectrum obtained in singles for the  $^{119}\text{Sn} + ^{40}\text{Ar}$  system by adding the single to sixfold  $0^\circ + 90^\circ$  spectra (solid line); calculated statistical spectrum (dotted line). (c) Spectra for  $^{154}\text{Er}$  (solid line) and  $^{155}\text{Er}$  (dot-dashed line). (d) Multiplicity spectra for the  $^{124}\text{Sn} + ^{40}\text{Ar}$  system (open squares) and  $^{119}\text{Sn} + ^{40}\text{Ar}$  system (filled squares). (e) Multipole spectra for  $^{124}\text{Sn}$  ( $^{119}\text{Sn}$ ) targets: stretched quadrupole component, open (filled) diamonds; stretched dipole components, crosses (pluses).

$^{159}\text{Er}$  products) gives a spectrum showing a characteristic rotational bump with a rather flat top up to around 1 MeV and extending up to about 1.6 MeV. The small peak at 550 keV corresponds to the backbending region well known in the  $^{160}\text{Er}$  residual nucleus. The  $^{119}\text{Sn} + ^{40}\text{Ar}$  case looks very different, having two very well separated peaks with a pronounced dip at 1 MeV. The low-energy bump has a high intensity and contains the heavily populated transitions around 700 keV which have been observed as discrete lines from states with spins up to  $36\hbar$  in  $^{154}\text{Er}$  and  $\frac{45}{2}\hbar$  in  $^{155}\text{Er}$ . The second bump starts at  $\sim 1$  MeV, and above the maximum (around 1.3 MeV), it seems to resemble rather closely the upper edge of the rotational bump observed with the  $^{124}\text{Sn}$  target. This second bump develops very strongly with increasing fold number, which shows that it contains transitions coming from high spins.

The multiplicity spectra have been obtained from the single to sixfold summed  $0^\circ + 90^\circ$  spectra, which are approximately independent of the multipole composition of the spectra. The multiplicity is calculated for each channel ( $\gamma$ -ray energy) using standard methods.<sup>5</sup> Figure 2(d) shows the multiplicity spectra obtained in singles [no Ge(Li) coincidence required] for the  $^{124}\text{Sn}$  and  $^{119}\text{Sn}$  targets. In the first case, the regular increase of multiplicity with transition energy reflects the rotational correlation between energy and spin. The rotational transition energy corresponding to the maximum spin is located at the upper edge of the bump in the  $\gamma$ -ray spectrum but the multiplicity drops there because of the increasing dilution by statistical  $\gamma$  rays which have the average multiplicity in the reaction.<sup>2</sup> The structure of the multiplicity spectrum is also very different in the  $^{119}\text{Sn} + ^{40}\text{Ar}$  system: There are two peaks corresponding to the two bumps observed in the  $\gamma$ -ray spectrum, and they are of equal height in spite of the much smaller intensity of the higher-energy bump in the  $\gamma$ -ray spectrum relative to the statistical component under it. We have tried to estimate quantitatively the multiplicity associated with the highest-energy part of this bump by subtracting a statistical component as shown in Fig. 2(b). This statistical part is normalized to the tail of the  $\gamma$ -ray spectrum at 2 MeV, which is close to the region of interest, and the multiplicity associated is the average value as found in the exponential tail region of the multiplicity spectrum. This increases by less than 1 unit (up to 27) the multiplicity in the lower bump region but brings up from 26 to about 31

the multiplicity associated with the high-energy part of the upper bump. The  $\gamma$  rays in this bump must then be associated with the highest multiplicity in the reaction, which means that they very probably come from the highest-spin states emitting  $\gamma$  rays. There is a remarkable similarity in the rise of the multiplicity in the  $^{124}\text{Sn} + ^{40}\text{Ar}$  and  $^{119}\text{Sn} + ^{40}\text{Ar}$  systems starting from the highest energy of the yrast region, which suggests a similar behavior of these two systems in this region.

The multipole composition of the  $\gamma$ -ray spectrum is deduced from the intensities observed in the  $0^\circ$  and  $90^\circ$  counters, under the assumption of only stretched dipole and quadrupole radiation. This assumption is likely to be generally correct for these very high-spin cases, but could in some regions be affected by other (or mixed) multipoles. The multipole spectra corresponding to the sum of threefold to sixfold spectra are shown channel by channel in Fig. 2(e) for the two systems again observed in singles. The total number of counts in these multipole spectra is normalized to the average multiplicity in the reaction. In the rotational case, there is, as expected, a strong predominance ( $\sim 75\%$ ) of stretched quadrupole transitions in the yrast region, in rather good agreement with previous data<sup>3</sup> though we find more stretched dipole transitions at low energy. The existence of such a strong, very low-energy dipole component in these rotational nuclei is an interesting unresolved problem at present. The most striking feature of the spectrum from the  $^{119}\text{Sn} + ^{40}\text{Ar}$  case is the very large predominance (80%) of stretched quadrupole transitions in the higher-energy bump. The multipole spectra of the two systems look similar in that energy region. In the lower part of the low-energy bump, there is a preponderance of stretched dipole transitions, whereas in the upper part of this bump (around 600 to 800 keV) there is a higher stretched quadrupole proportion. This is in agreement with the known discrete lines in  $^{154}\text{Er}$  and  $^{155}\text{Er}$ .

The Ge(Li) coincidence spectra have been used to look for differences between  $4n$  and  $5n$  residual products. The two products  $^{160}\text{Er}$  and  $^{159}\text{Er}$  behave similarly, but  $^{159}\text{Er}$  does not backbend in this region, and therefore has no peak at 550 keV. Also, for this nucleus, the yrast rotational bump does not extend to as high energies as in  $^{160}\text{Er}$ , because of the fractionation of angular momentum left in the residual nuclei: The heavier product ( $4n$  here) has the higher angular mo-

mentum. In Fig. 2(c), the  $0^\circ$  spectra are shown (summed over zero to sixfold) in coincidence with the known lines of the  $4n$  ( $^{155}\text{Er}$ ) and  $5n$  ( $^{154}\text{Er}$ ) products. They both have an intense low-energy bump though these differ in detail. The higher-energy bump appears to be located mostly in  $^{155}\text{Er}$  which is the  $4n$  product. However, such transitions deexcite states with the highest spins, which are not expected to be populated in the  $5n$  product. Thus, this reduction of the higher bump in  $^{154}\text{Er}$  probably does not reflect a difference in the structure of these nuclei at high spins, but is simply an angular momentum fractionation effect.

Of the two bumps observed in the  $^{119}\text{Sn} + ^{40}\text{Ar}$  system, the lower contains the previously known transitions extending up to about 1 MeV (and  $36\hbar$  in the case of  $^{154}\text{Er}$ ), and in the spectra before compression it is easy to identify these lines (or groups of lines). It is surprising that these spectra are so strongly dominated by the known (yrast) lines, but that is, of course, the reason why it has been possible to see them individually as discrete lines. Even more surprising is the sharp cutoff in energy of these lines at  $\sim 1$  MeV, since we might expect a rather broad distribution scattered around the average value given by the rigid-sphere moment of inertia<sup>6</sup> which would be 1 MeV for spin  $35\hbar$ . We do not understand why the lines from such weakly collective regions should be so sharply confined in energy, but those previously known were, and the present spectra show that there are not many others of this type extending higher in energy. It is this cutoff that makes the second collective bump so apparent.

The properties of the high-energy bump suggest that the erbium nuclei around  $N = 86$  are strongly collective (very probably rotational) at the highest spin values. The strong predominance of stretched  $E2$  transitions is a characteristic feature of collective behavior and values as high as 80% have only been found in similar continuum studies in regions thought to be rotational.<sup>3</sup> Furthermore, the transition energies are appropriate for a rotational behavior. The maximum spin at the top of  $\gamma$  cascade in the  $^{119}\text{Sn} + ^{40}\text{Ar}$  system is calculated<sup>2</sup> from the bombarding energy to be about  $60\hbar$ . Together with a maximum energy in the bump of 1.6 MeV (best defined as the midpoint of the fall of the multiplicity peak), this gives a moment of inertia of  $150 \text{ MeV}^{-1}$  which is reasonable for this mass region (the estimated uncertainty is 10% for the spin and also for the  $\gamma$ -ray energy, giving about 15% in the moment of inertia). Using this moment of

inertia for the 1.1-MeV lower-energy edge of the bump gives a spin of  $40\hbar$  for this point, which coincides with the end of the observed noncollective transitions. Finally, this type of behavior is suggested by the similarity in this energy region of both the  $\gamma$ -ray spectrum and the multiplicity spectrum to those for the  $^{159,160}\text{Er}$  nuclei which have been shown to be rotational up to the highest spins. Thus there is reasonably good evidence that the structure of  $^{155}\text{Er}$  and  $^{154}\text{Er}$  nuclei changes from a spherical or weakly oblate one at spins below  $\sim 40\hbar$  to a highly collective (very likely rotational) one above that spin. We cannot exclude the possibility that part of the population above spin  $40\hbar$  still feeds weakly collective states which might continue the yrast sequence observed below spin  $40\hbar$ , but we have no evidence for this, and the lack of transitions around 1 MeV which would extend the low-energy bump makes it seem unlikely to us. The proposed change of structure could very nicely explain this limit to the discrete lines.

The type of rotational behavior in these nuclei is not so clear. The theoretical calculations<sup>7</sup> predict oblate ( $\beta \sim -0.2$ ) or strongly prolate ( $\beta \simeq 0.6$ ) deformations at very high spins in these nuclei. It is possible that we are seeing the rotational transitions from an oblate nucleus rotating about an axis perpendicular to the symmetry axis. In the absence of shell effects, such nuclei would have a moment of inertia smaller than the rigid-sphere value  $\mathcal{I}_0$  [ $\mathcal{I} \simeq \mathcal{I}_0(1 - 0.3\beta)$ ]. On the other hand, the moment of inertia estimated above is 15% larger than the rigid-sphere value, making the prolate shape somewhat more probable. The moment of inertia estimated in a similar way for the  $^{159,160}\text{Er}$  nuclei is  $\mathcal{I} \simeq 130 \text{ MeV}^{-1}$ , slightly less than the rigid-sphere value. Since these nuclei are believed to be prolate at all spin values, the larger moments of inertia for the  $^{154,155}\text{Er}$  system are reasonable strong evidence that they are also prolate. Prolate deformations of  $\beta = 0.6$  would imply moments of inertia about 1.6 times larger than the rigid-sphere value, which is also rather far from the observed values. For a prolate nucleus, a moment of inertia 15% larger than the rigid-sphere value would imply  $\beta \sim 0.3$ . Thus, it seems most likely to us that these  $^{154,155}\text{Er}$  nuclei are prolate with deformations comparable to, or slightly larger than, the heavier rotational rare-earth nuclei.

(<sup>a</sup>)Permanent address: Lawrence Berkeley Laboratory,

Berkeley, Cal. 94720.

<sup>1</sup>T. L. Khoo, R. K. Smith, B. Haas, O. Häusser, H. R. Andrews, O. Horn, and D. Ward, *Phys. Rev. Lett.* **41**, 1027 (1978); C. Baktash, E. der Mateosian, O. C. Kistner, and A. W. Sunyar, *Phys. Rev. Lett.* **42**, 637 (1979); P. Auger *et al.*, *Z. Phys.* **A285**, 59 (1978); P. Auger *et al.*, *J. Phys. G* **3**, 157 (1977).

<sup>2</sup>M. A. Deleplanque, I. Y. Lee, F. S. Stephens, R. M. Diamond, and M. M. Aleonard, *Phys. Rev. Lett.* **40**, 629 (1978).

<sup>3</sup>M. A. Deleplanque, Th. Byrski, R. M. Diamond, H. Hübel, F. S. Stephens, B. Herskind, and R. Bauer,

*Phys. Rev. Lett.* **41**, 1105 (1978).

<sup>4</sup>R. S. Simon, M. V. Banaschik, R. M. Diamond, J. O. Newton, and F. S. Stephens, *Nucl. Phys.* **A290**, 253 (1977).

<sup>5</sup>G. B. Hagemann, R. Broda, B. Herskind, M. Ishihara, S. Ogaza, and H. Ryde, *Nucl. Phys.* **A245**, 166 (1975).

<sup>6</sup>A. Bohr and B. R. Mottelson, *Nuclear Structure* (Benjamin, New York, 1975), Vol. II, p. 81.

<sup>7</sup>T. Døssing, K. Neergård, K. Matsuyanagi, and Hsi-Chen Chang, *Phys. Rev. Lett.* **39**, 1395 (1977); G. Leander, private communication.

## Shape-Resonance-Enhanced Nuclear-Motion Effects in Molecular Photoionization

J. L. Dehmer

*Argonne National Laboratory, Argonne, Illinois 60439*

and

Dan Dill and Scott Wallace<sup>(a)</sup>

*Department of Chemistry, Boston University, Boston, Massachusetts 02215*

(Received 5 July 1979)

Shape resonances in molecular photoionization are shown to induce strong coupling between vibrational and electronic motion over a spectral range several times broader than the resonances half-width. This coupling is manifested by large deviations from Franck-Condon intensity distributions and strong dependence of photoelectron angular distributions on the vibrational state of the residual ion. These effects are illustrated for the  $3\sigma_g$  photoionization channel of  $N_2$ .

Molecular photoionization at wavelengths unaffected by autoionization, predissociation, or ionic thresholds is generally believed to produce Franck-Condon (FC) vibrational intensity distributions and  $v$ -independent photoelectron angular distributions. In this Letter, we predict that the shape resonances being identified<sup>1-7</sup> in the spectra of a growing, diverse collection of molecules represent an important class of exceptions to this picture. In particular, the temporary trapping of the photoelectron by a centrifugal barrier enhances the coupling between electronic and vibrational motion, leading to striking non-FC intensities and strongly  $v$ -dependent asymmetry parameters over a broad spectral range encompassing the resonance. We illustrate these ideas with a calculation of the  $3\sigma_g$  photoionization channel of  $N_2$ , which exhibits the well-known  $\sigma_u$ ,  $f$ -wave shape resonance.<sup>2,4-6,8-18</sup> In addition to predicting non-FC vibrational branching ratios, we account for the long unexplained observation<sup>19</sup> that the  $\beta$  values for production  $N_2^+ X^2\Sigma_g^+(v=0, 1)$  differ significantly at 584 Å (and other wavelengths), where

none of the more traditional mechanisms mentioned above apply. We believe that this illustration for  $N_2$  is merely the first of many examples of shape-resonance-enhanced nuclear-motion effects which have hitherto gone undetected only because vibrationally resolved photoelectron studies have not been carried out systematically through molecular shape resonances, as is now possible with synchrotron-radiation sources.

The breakdown of the FC principle arises from the quasibound nature of the shape resonance, which is localized in a spatial region of molecular dimensions by a centrifugal barrier. This barrier and, hence, the energy and lifetime (width) of the resonance are sensitive functions of internuclear separation  $R$  and vary significantly over a range of  $R$  corresponding to the ground-state vibrational motion. This is illustrated in the upper portion of Fig. 1 where the dashed curves represent separate, fixed- $R$  calculations of the partial cross section and asymmetry parameter for  $N_2$   $3\sigma_g$  photoionization over the range  $1.824a_0 \leq R \leq 2.324a_0$ , which spans the  $N_2$  ground-